Atomic and electronic structure of the diamond (100) surface: Reconstructions and rearrangements at high hydrogen coverage

M. D. Winn,* M. Rassinger, and J. Hafner
Institut für Theoretische Physik, Technische Universität Wien, Wiedner Hauptstraße 8-10, A-1040 Wien, Austria
(Received 25 July 1996)

The atomic and electronic structure of the diamond (100) surface has been investigated theoretically via a semiempirical tight-binding model for a range of hydrogen coverages. Model parameters for C-C interactions have been taken from the work of Goodwin [J. Phys. Condens. Matter **3**, 3869 (1993)], while new parameter sets have been determined for C-H and H-H interactions. The model gives results for the clean and monohydrogenated surfaces in good agreement with previous studies, but different features have been identified for higher H coverages. When the H coverage is sufficiently high, the substrate lattice is found to distort in order to reduce steric repulsions between dihydride units. As an important example, we obtain two structures for the dihydrogenated surface that are significantly more stable than those proposed previously. For H coverages intermediate between the monohydrogenated and dihydrogenated surfaces, stable geometries consisting of monohydrogenated dimer units and dihydride units are found. In contrast, geometries that include isolated monohydride units, such as have been previously investigated, are found to be thermodynamically and kinetically unstable. Tight-binding molecular dynamics is used to illustrate a mechanism for the rapid removal of isolated monohydride units. The electronic structures of the surfaces are described via the total and partial electronic densities of state, which are obtained directly from the tight-binding Hamiltonian. For the monohydrogenated surface and higher coverages, the stable geometries are found to yield no states in the bulk band gap. [S0163-1829(97)06608-3]

I. INTRODUCTION

Diamond surfaces are presently the subject of intense international research, both as a test of the current theoretical understanding of wide band-gap semiconductors and because of their technological importance. Due to its favorable mechanical and thermal properties, diamond has been suggested as a suitable material for a number of applications involving extreme conditions, including its use as a possible replacement for silicon in electronic devices. The realization of this aim has been advanced by the technique of chemical vapor deposition (CVD),[1] with which diamond films can be grown easily and rapidly *in situ*. The principal products of diamond film growth via CVD are (100) and (111) facets, and thus the microscopic processes occurring at C(100) and C(111) surfaces are of particular interest.

In the present paper, we are concerned with the atomic structure, electronic structure, and dynamic properties of C(100) terraces. In addition to its appearance in CVD-grown diamond films, the C(100) surface is unique among the low-index surfaces in having two dangling bonds per surface atom, leading to a variety of bonding possibilities, and a rich and varied surface chemistry. Central to an understanding of any carbon surface is the role of adsorbed hydrogen, and so particular attention is paid to the effects of different H coverages. When fully saturated by hydrogen, the number of adsorbed H atoms per surface C atom (the coverage, θ) for the (100) surface is two.

Despite intensive study, an overall consensus on the microscopic structure of the C(100) surface in the presence of hydrogen has not yet been reached. That the bare C(100) surface undergoes a reconstruction, forming rows of surface dimers and giving a (2×1) pattern in low-energy electron diffraction (LEED) experiments,[2,3] is now established beyond reasonable doubt. Of the various possible hydrogenated surfaces, the monohydrogenated surface ($\theta=1$) is certainly the best understood, with all theoretical studies[4–14] predicting surface dimers with one H atom bonded to each constituent C atom, again giving a (2×1) LEED pattern. Higher coverages have also been studied by theory [$\theta=1.33$ (Refs. 6, 8, and 14), $\theta=1.5$ (Refs. 7,10–12, and 14) and $\theta=2$ (Refs. 4,6,9,10,13, and 14)], but there is some disagreement on the structure and relative stability of these high H coverage surfaces.

The evidence from experiment with regard to the degree of H coverage and the corresponding surface structure that predominates under different conditions is conflicting. Typically, annealing of a cleaned and polished diamond sample to a temperature $T<1000$ K yields a (1×1) symmetry, as observed by LEED.[15–18] On heating the sample to $T\sim1400$ K, a surface reconstruction takes place producing a (2×1) LEED pattern[15–18] and correlating with the desorption of hydrogen.[15] Scanning tunnelling microscopy (STM) studies[7,19] confirm the (2×1) reconstruction, and show rows of surface dimers. Hamza *et al.*[15] and Lee and Apai[17] found that the (1×1) pattern could be recovered by dosing the sample with atomic H or D. In contrast, Thomas *et al.*[16] and Smentkowski *et al.*[18] found that the (2×1) pattern persisted even for very heavy dosing. It is perhaps noteworthy that oxygen, which is a common impurity, appears to stabilize the (1×1) symmetry[15,16]—possible atomic structures in the presence of adsorbed O have been given by Thomas *et al.*[16]

The low-temperature (1×1) structure is generally assumed[15,18] to be the dihydrogenated ($\theta=2$) surface, con-

sisting of the bulk diamond structure with the dangling bonds passivated by hydrogen. Hamza *et al.*[15] assigned the (2×1) structure produced by annealing at high temperature to the monohydrogenated ($\theta=1$) surface, based on the continued presence of the ''slow'' proton peak in electron stimulated desorption (ESD) experiments. However, high-resolution electron-energy-loss spectroscopy (HREELS) experiments on the high-temperature (2×1) structure[17,18,20] have failed to find significant features corresponding to C-H vibrations, and these authors have concluded that the surface is hydrogen free. Lee and Apai[17] deduced from their HREELS results a number of aliphatic and olefinic CH_x surface species for the low-temperature (1×1) surface that they observed. In contrast, Thoms and Butler[20] and Smentkowski *et al.*[18] observed a (2×1) structure on dosing with H or D at low temperature, and concluded from HREELS experiments that the surface was monohydrogenated. Thoms and Butler[20] suggested that the extra species identified by Lee and Apai[17] were assignable to steps and defects on the surface.

The valence-band electronic structure has been studied via ultraviolet photoelectron spectroscopy (UPS).[15,21–23] On annealing the diamond samples at high temperature, filled surface states appear in a 1.5-eV-wide range immediately above the valence-band maximum.[15,21,23] Angle-resolved measurements reveal there to be two surface states in this energy range, each possessing a moderate dispersion.[21,23] Exposure to atomic deuterium causes these surface features to disappear almost completely.[23] Exposure to very high doses of hydrogen or deuterium results in further changes in the electronic spectrum. The features have tentatively been attributed to the presence of CH_2 and CH_3 fragments at the surface.[22] Two-photon UPS with pump photon energies in the range 1.2–5.5 eV failed to reveal any empty states in the bulk diamond band gap for either the low-temperature (1×1) or the high-temperature (2×1) surface.[15] Hamza *et al.*[15] concluded from the absence of empty π^* states in the bulk band gap that the UPS measurements of the high-temperature surface were consistent with the $\theta=1$ assignment. In contrast, Wu *et al.*[21] and Francz and Oelhafen[23] concluded from the filled surface states that the high-temperature surface was the clean C(100) surface.

It seems probable therefore that the C(100) surface annealed at $T\sim1400$ K corresponds to $\theta=0$ or possibly $\theta=1$. It is less clear whether the equilibrium coverage at low temperatures is $\theta=1$ or $\theta>1$. In any case, it is likely that as-prepared CVD diamond samples do correspond to large θ, even if they are thermodynamically metastable. Furthermore, regions of high H coverage may occur as intermediates during CVD growth.[32] Given the possible role of $\theta>1$ coverages, and the theoretical uncertainty regarding the corresponding stable atomic structures and associated properties, it seems worthwhile to reexamine these surfaces.

Before we present the results of our study, it is also interesting to review very briefly the influence of hydrogen on the (100) surfaces of silicon and germanium. For both elements, the best characterized surfaces are again the clean and monohydrogenated (2×1) surfaces. However, unlike clean C(100) with symmetric and unbuckled surface dimers, for Si(100) there is conflicting evidence indicating either symmetric or asymmetric dimers,[24,25,27,26] and for Ge(100) asymmetric buckled dimers are definitely preferred.[28] Recent *ab initio* studies[2,11,12] relate the absence of buckling on the C(100) surface to the large bonding-antibonding splitting of the surface states that makes the Jahn-Teller-like symmetry breaking observed on the Si and Ge surfaces energetically unfavorable. Hydrogenation eliminates the symmetry breaking also on the (2×1) Si(100):H surface.[29] On hydrogenated Si(100):nH surfaces, Sakurai and Hagstrum[30] also observed a (1×1) phase that was tentatively associated with a symmetric dihydride structure, and Chabal and Raghavachari[31] discovered a (3×1) phase described as an ordered mixture of monohydride and dihydride units. Northrup[29] has calculated the stability of the (1×1), (2×1), and (3×1) H-terminated Si(100) surfaces as a function of the hydrogen chemical potential and predicted that all three phases can be found over a certain range of the chemical potential. For the (1×1) phase, however, the lowering of the energy resulting from the formation of a canted dihydride structure was found to be essential for understanding the stability of this phase. This could also be a realistic scenario for the hydrogenated C(100) surfaces.

Here we present the results of a detailed theoretical study of C(100) surfaces with H coverages in the range $1<\theta\leqslant2$, using an accurate and computationally efficient semiempirical tight-binding model (TBM). The TBM is introduced and described in detail in Sec. II. A particular advantage of the TBM is its computational efficiency, which allows the study of relatively large systems, and perhaps more importantly for the present study a large number of bonding scenarios. This efficiency stems from the use of simple parametrized matrix elements, and we describe and comment on the chosen functional forms and associated parameters. The transferability of the model is tested by a comparison with the known geometries of a number of small hydrocarbon molecules and the established structures of the $\theta=0$ and $\theta=1$ surfaces.

In Sec. III, we begin the presentation of results with the atomic structures predicted by the model. A major issue for high H-coverage surfaces is the steric repulsion that exists between neighboring bonded H atoms. For all $\theta>1$, a fraction of the surface C atoms must be bonded to two H atoms, forming dihydride (methylene) units. Steric repulsion between neighboring dihydride units makes an unfavorable contribution to the total energy, and this contribution becomes more important as the H coverage increases. The $\theta=2$ surface is the most extreme case, and it is for this reason that the dihydrogenated surface has often been rejected as unlikely to occur. One important result of our study is that there exists a reconstruction of the $\theta=2$ surface for which the steric repulsion is minimized, making this surface more stable than previously thought.

The valence electronic density of states and atomic-orbital-resolved partial densities of state can be obtained directly from the TBM. We give in Sec. IV the densities of state corresponding to the structures presented in Sec. III. In contrast to some earlier studies,[7,11,12] we predict that there are no surface states in the bulk band gap for all coverages $\geqslant1$.

Growth via CVD is likely to lead to transient or metastable structures, and so we are also interested in dynamic processes occurring at the C(100) surface. Tight-binding molecular dynamics (TBMD), in which the forces at each time step are calculated exactly from the TBM,[33] has recently

become a popular technique. In the present study, we have applied TBMD to study a particular transformation of a surface from a metastable to a stable atomic configuration at a temperature typical of CVD. Results are given in Sec. V. Finally, some closing remarks are given in Sec. VI.

II. TIGHT-BINDING MODEL AND PARAMETRIZATION

Within the local-density approximation to electronic exchange and correlation interactions and a tight-binding approach, the total potential energy E for a given atomic configuration can be expressed in terms of a band energy, equal to a sum over the eigenenergies ϵ_ν of occupied valence electronic states, plus a sum over repulsive pair potentials $V_{\rm rep}(r)$ (Ref. 34)

$$E=\sum_{\nu_{\rm occ}} \epsilon_\nu+\sum_{ij} V_{\rm rep}(r_{ij}), \tag{1}$$

where r_{ij} is the internuclear separation of atoms i and j. The pair-interaction term describes the electrostatic interactions and accounts in addition for the double-counting and nonorthogonality corrections. The electronic eigenenergies ϵ_ν are obtained by diagonalizing the TB Hamiltonian $H_{\rm TB}$, which is expressed in a basis of localized orbitals associated with the individual atoms. We adopt the standard minimal basis, consisting of one s orbital and three p orbitals on each C atom, and a single s orbital on each H atom (cf. the work of Gavrilenko[9] who included an extra s^* orbital on each C).

The potential energy E is thus determined by the diagonal and off-diagonal elements of $H_{\rm TB}$ [ϵ_α and $t_{\alpha\beta}(r)$ respectively, where α, β denote basis orbitals] and by $V_{\rm rep}(r)$. The r dependence of the intersite terms $t_{\alpha\beta}$ and $V_{\rm rep}$ is assumed to follow the scaling form of Goodwin *et al.*,[35] namely a power law decay modulated by a smoothed step function located at r_c and with a sharpness determined by n_c:

$$s(r)=s(r_0)\left(\frac{r_0}{r}\right)^m \exp\left\{m\left[-\left(\frac{r}{r_c}\right)^{n_c}+\left(\frac{r_0}{r_c}\right)^{n_c}\right]\right\}. \tag{2}$$

Here, $s=t_{\alpha\beta}$ or $V_{\rm rep}$, $m=m_{\rm t}$ or $m_{\rm V}$, and r_0 is the equilibrium internuclear separation.

In order to avoid time-consuming calculations, we do not include explicit Coulomb terms in the total potential-energy function. Such terms are often introduced to reduce unphysical charge transfer, either via a positive contribution to the total energy related to the deviation from charge neutrality,[10] or via a self-consistent adjustment of the diagonal matrix elements.[9,36] In fact, we find charge transfer, as estimated by the Mulliken population, to be small in all situations studied (typically $< 0.1e$). Even for the extreme case of the H-atom migration shown in Fig. 8, the charge transfer does not exceed $0.15e$. Note that the lack of significant charge transfer is to some extent due to the values we have chosen for the (fixed) diagonal matrix elements; see below.

For a given atomic configuration, we construct the Hamiltonian matrix and diagonalize it exactly to obtain the electronic eigenenergies ϵ_ν and eigenfunctions. The temperature of the electronic subsystem is assumed to be zero, so that the lowest $N_e/2$ eigenstates are occupied, where N_e is the number of valence electrons. The total energy is then obtained directly from Eq. (1). An analytical expression for the total force on each atom can be obtained by taking the appropriate derivative of Eq. (1). The contribution from the band energy term follows from the Hellmann-Feynman theorem, and requires derivatives of the Hamiltonian matrix elements and the coefficients of the occupied eigenstates (see Ref. 33 for details).

With the atomic forces thus calculated, we search for minima of the potential-energy surface using a conjugate gradient (CG) algorithm. The particular minimum found is obviously influenced by the chosen starting atomic configuration. In an attempt to locate all relevant minima, and in particular the absolute minimum, we have investigated a number of different starting configurations for each H coverage. A starting configuration typically consists of a particular deformation of the ''ideal'' structure, with some asymmetry added in order to avoid being trapped in a prespecified symmetry. The ability to explore a range of starting conditions is a consequence of the computational speed of the chosen semiempirical approach.

A knowledge of the atomic forces also allows one to investigate the dynamics of the system via molecular-dynamics simulations in the microcanonical ensemble. We have used a fourth-order Gear predictor-corrector algorithm[37,38] with a time step of 1 fs to integrate the equations of motion of the atomic coordinates. Molecular-dynamics simulations based on a TB expression for the potential energy have recently become popular for carbon and silicon systems (see, e.g., Refs. 33, 39 and 40 and references therein). In addition to the generation of atomic trajectories at finite temperatures, TBMD simulations were also used to generate approximate starting configurations for the CG algorithm via a simulated annealing approach.

For a practical implementation of the model, we must determine parameter sets for C-C, C-H, and H-H interactions. The C-C parameters are taken to be those of Goodwin[41] (see Table I), who fitted the values of ϵ_α and $t_{\alpha\beta}(r_0)$ to the band structure of the equilibrium diamond lattice,[44] while the remaining parameters are fitted[41] to the equilibrium volume of the diamond lattice, the diamond-graphite equilibrium energy separation, the bulk modulus of diamond, and the face-centered cubic equilibrium volume. The Goodwin parametrization is found to give results similar to those of Xu *et al.*[42] for the clean diamond surface and for liquid carbon,[43] while retaining the straightforward pair potential form for the repulsive contribution to the energy.

Alternative parameter sets have been developed for the C-H and H-H interactions. The H-H parameters were obtained by fitting the results of the TBM to the *ab initio* binding-energy curve of the H_2 molecule calculated by Kolos and Wolniewicz[45] (note that at the level of accuracy of the current application, there is no significant difference between the various calculations reported in Ref. 45). A good fit is obtained in the vicinity of the equilibrium internuclear separation $r_0=0.742$ (namely, in the range $0.5\ \text{Å}<r<1.3\ \text{Å}$) but, as is appropriate for bulk phase applications, the interactions were made to drop off more rapidly than they do in the H_2 molecule by an appropriate choice of the cutoff parameters r_c and n_c. The resulting H-H parameter set is given in Table I. In contrast, Davidson and Pickett[10] evaluated the H-H parameters from the interaction between H atoms located on different methane molecules, having in mind the

TABLE I. Parameters of the tight-binding model; see text for key. Energies are given in eV, and lengths in angstroms.

	ϵ_s	ϵ_p	$t_{ss\sigma}(r_0)$	$t_{sp\sigma}(r_0)$	$t_{pp\sigma}(r_0)$	$t_{pp\pi}(r_0)$	$V_{\rm rep}(r_0)$
C-C	−5.16331	2.28887	−4.43338	3.78614	5.65984	−1.82861	10.92
C-H			−4.81	5.32			7.923
H-H	0.42583		−6.374				8.0
	$m_{\rm t}$	$m_{\rm V}$	r_0	$r_{\rm c}$	$n_{\rm c}$		
C-C	2.796	4.455	1.536	2.32	22		
C-H	1.949	3.372	1.094	2.0	22		
H-H	1.59	2.52	0.742	1.5	8		

repulsion between bonded H atoms on the diamond surface. We believe our procedure to be more general, and that steric repulsions between bonded surface H atoms should arise naturally from the properties of a fully saturated bonding network.

The diagonal matrix element ϵ_s of H atoms, which is obviously undetermined by the above fitting, was fixed at the C sp^3 hybridization energy $(\epsilon_s+3\epsilon_p)/4$, in order to minimize charge transfer in typical bonding situations. As mentioned above, this aim appears to be fulfilled. Having thus fixed all of the H-H parameters, the C-H parameters were fitted to the binding energy, equilibrium bond length, and vibrational frequencies of CH_4 (experimental values have been taken from the compilations in Refs. 46 and 47). The parameters adopted are displayed in Table I.

As a preliminary test of the TB model, we consider a small selection of hydrocarbon molecules that exemplify the sp^3 and sp^2 hybridization likely to be of relevance to diamond surfaces. Sample results are given in Table II. Although the predicted geometry does not agree perfectly with experiment, the major trends are reproduced, notably the shortening of the C–C bond in going from alkane to aromatic ring to alkene. It must also be remembered that quoted experimental bond lengths sometimes differ by up to 0.01 Å, depending on the source and method used. The calculated values of the atomization energy E_B are in excellent agreement with the experimental values quoted in Ref. 46, which is of course a direct consequence of the fitting procedure discussed above. Finally, from the values of q_H shown in Table II it is clear that charge transfer is small, giving *a posteriori* justification for the neglect of Coulomb terms.

The results presented in Secs. III and IV for the static properties of hydrogenated diamond surfaces were obtained using a slab geometry consisting of 12 carbon layers and 8

TABLE II. Comparison of the TB model with experiment for selected properties of small hydrocarbon molecules. Bond lengths are given in angstroms. E_B is the atomization energy of the molecule in eV and $q_{\rm H}$ is the calculated charge on an H atom given in units of the electronic charge. Experimental values for bond lengths and angles are taken from Ref. 47. Experimental values for E_B are those quoted in Ref. 46.

			C_2H_6		
	r(C-C)	r(C-H)	∠CCH (degrees)	E_B	q_H
Present work	1.506	1.098	109.5	30.985	−0.04
Experiment	1.535	1.094	111.2	30.90	
			C_3H_8		
	r(C-C)	r(C-H)	∠CCC (degrees)	E_B	q_H
Present work	1.514	1.097 and 1.102	109.6	43.758	−0.04
Experiment	1.532	1.107	112	43.3	
			C_2H_4		
	r(C-C)	r(C-H)	∠CCH (degrees)	E_B	q_H
Present work	1.345	1.089	120.4	24.116	+0.02
Experiment	1.339	1.087	121.3		
			C_6H_6		
	r(C-C)	r(C-H)	E_B	q_H	
Present work	1.407	1.088	58.161	+0.03	
Experiment	1.399	1.101			

atoms per layer in a (4×2) surface cell. Periodic boundary conditions are applied in the x and y directions (orientated along [011] and [011] with respect to the crystallographic axes), with two free surfaces in the z direction. We note that the surface cell is large enough to allow for higher-order reconstructions than (2×1). Hydrogen atoms are added to both surfaces to give the required coverage, and all atoms are free to move. All energies quoted are per surface site (SS), of which there are 16. The TBMD simulations reported in Sec. V used an identical geometry, except that the number of layers was restricted to 8 in the interest of speed. The size and orientation of the surface of the simulation cell obviously influence the H coverages and geometries that can be studied. The present choice of a 4×2 surface cell is, we think, sufficient to reveal the basic trends for fractional H coverage.

Sample calculations were also performed with between 6 and 16 carbon layers in order to test the convergence of the results with respect to slab thickness. Quantities such as bond-lengths show oscillatory convergence, the oscillation of period-4 layers arising from the symmetry of the diamond lattice in the [100] direction. We find the results to be satisfactorily converged at a thickness of 12 layers—in all cases bond lengths changed by less than 0.001 Å in going from a 12-layer to a 16-layer calculation. In contrast, bond lengths changed by up to 0.01 Å when an 8-layer slab was used. For the TBMD simulations, this was deemed not to be a problem, since deviations in the bond lengths arising from thermal motion are in any case larger.

With stable atomic configurations determined by CG minimization, we can also investigate the valence electronic structure of the system of interest. Diagonalization of the TB Hamiltonian leads directly to the electronic eigenenergies, from which we deduce the density of states (DOS) of the occupied valence and unoccupied conduction bands. In order to improve the representation of the electronic bands, we performed k-point sampling in the x-y plane using 16 special k points from the Monkhorst-Pack scheme.[48] In addition a Gaussian smearing with a mean-square deviation of $0.05/\sqrt{2}$ eV was used to produce a smoother DOS. Using the eigenvector coefficients, we can also calculate various partial densities of state, from which an idea of the nature and spatial extent of the eigenstates can be obtained (see Sec. IV).

Before we present the principal results of this paper concerning high H-coverage surfaces, we briefly describe the predictions of the model for the bare and the monohydrogenated surfaces. A CG minimization for the bare surface ($\theta=0$) yields symmetric surface dimers of length $R_{\text{C-C}}=$ 1.406 Å, and a reconstruction energy relative to the terminated bulk structure of $\Delta E=-1.513$ eV/SS. Self-consistent *ab initio* local-density-approximation (LDA) calculations predict a dimer length of $R_{\text{C-C}}=1.37$ Å for symmetric dimers,[2,11–14,49] non-self-consistent TB-LDA calculations based on the Harris-Foulkes functional $R_{\text{C-C}}=1.40$ Å for buckled dimers.[8] The *ab initio* value for the reconstruction energy is $\Delta E=-1.51$ eV/SS.[12] For the monohydrogenated surface, ($\theta=1$) we obtain a symmetric dimer of length $R_{\text{C-C}}=$ 1.600 Å, a C-H bondlength of $R_{\text{C-H}}=1.098$ Å, and a hydrogen adsorption energy relative to the bare surface plus hydrogen atoms of $\Delta E_{\text{H}}=-4.049$ eV/SS. The predicted geometry is again in good agreement with *ab initio* results[8,11–14] ($R_{\text{C-C}}=$ 1.61 and 1.67 Å, $R_{\text{C-H}}=$ 1.10 and 1.17 Å in the self-consistent[12] and non-self-consistent[8] calculations, respectively), but the adsorption energy is slightly lower than the *ab initio* values of -6.20 eV/SS (Ref. 8) and -5.436 eV/SS.[11,12] We expect, therefore, the TBM to give reliable geometries and reasonable estimates of energy changes.

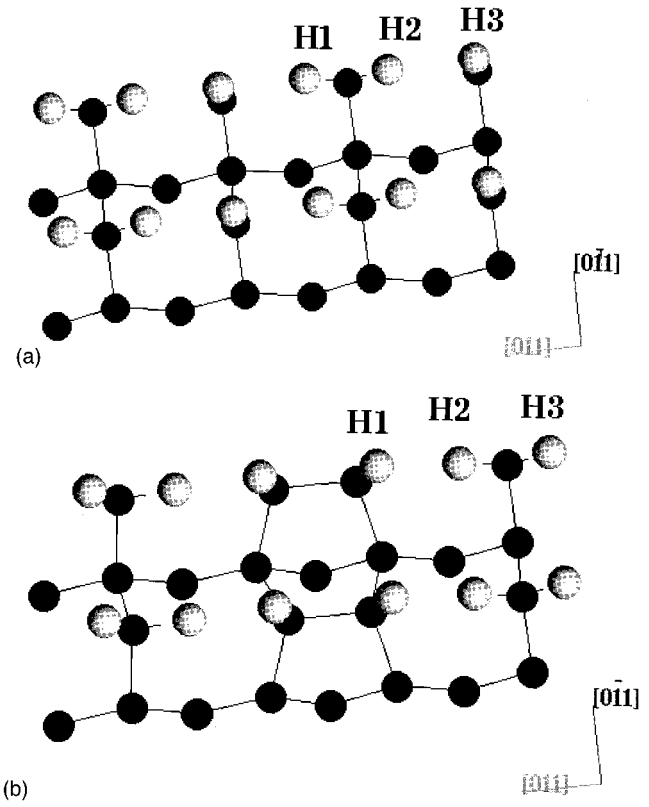

FIG. 1. Views of (a) a metastable and (b) the stable structure of C(100):1.5H, as obtained by CG minimization. C (H) atoms are shown in black (white), and only the upper three carbon layers are displayed. Selected bond lengths are given in Table III. Atoms H1, H2, and H3 are for later reference (see Fig. 8 and accompanying text).

III. EQUILIBRIUM ATOMIC STRUCTURES

In Fig. 1, we show two different structures for the $\theta=1.5$ surface, both obtained by CG minimization but starting from different trial configurations. Selected bond lengths are compared in Table III with the results of *ab initio* calculations. The structure of Fig. 1(a) consists of alternating rows of dihydride and monohydride units with (2×1) periodicity in the adsorbed hydrogen layer, and is the structure assumed in the studies of Refs. 7, 11, 12, and 14. The quantitative agreement with the latter is good, in particular with the *ab initio* studies[11,12,14] in which the C-H bond length is also found to be longer for the dihydride unit.

We find, however, that the structure shown in Fig. 1(a) is only metastable, lying 1.046 eV/SS above the alternative structure shown in Fig. 1(b). In the latter, the monohydride units are placed in adjacent positions, whence a surface dimer readily forms, removing the dangling bonds of the monohydride units. This results in a (4×1) periodicity of

TABLE III. Comparison of surface geometries. Bond lengths are given in angstroms.

	C(100)(2×1)			
	$R_{C\text{-}C}$ (dimer)	$R_{C\text{-}C}$ (back bond)		
Present work	1.406	1.538		
Ref. 11	1.37	1.50		
	C(100)(2×1):H			
	$R_{C\text{-}C}$ (dimer)	$R_{C\text{-}C}$ (backbond)	$R_{C\text{-}H}$ (dimer)	
Present work	1.600	1.549	1.098	
Ref. 11	1.61	1.53	1.10	
	C(100):1.25H			
	$R_{C\text{-}C}$ (dimer)	$R_{C\text{-}H}$ (dimer)	$R_{C\text{-}H}$ (dihydride)	
Present work	1.584	1.098	1.087	
	C(100):1.5H			
	$R_{C\text{-}C}$ (dimer)	$R_{C\text{-}H}$ (dimer)	$R_{C\text{-}H}$ (dihydride)	$R_{C\text{-}H}$ (monohydride)
Present work (dimers) [a]	1.548	1.099	1.087	
Present work (Altern.) [b]			1.110	1.089
Ref. 11 (Altern.)			1.11	1.09
Ref. 14 (Altern.)			1.11	1.09
	C(100):1.75H			
	$R_{C\text{-}C}$ (dimer)	$R_{C\text{-}H}$ (dimer)	$R_{C\text{-}H}$ (dihydride)	
Present work	1.572	1.099	1.132 & 1.093	
	C(100):2H			
	Twist (degrees)	Canting (degrees)	$R_{C\text{-}H}$ (dihydride)	∠H-C-H (degrees)
Present work (lean-to)[c]			1.114	94.3
Present work (herring-b.)[d]			1.123	93.7
Present work (twisted)[e]	33.0	0	1.147	90.5
Present work (id.)[e]	0	0	1.113	77.1
Ref. 10 (id.)	0	0	1.07	
Ref. 14 (id.)	0	0	1.05	83
Ref. 14 (canted)[e]	0	11	1.11,1.05	91
Ref. 14 (twisted)[e]	19	0	1.07	86
Ref. 13 (id.)[e]	0	0	1.06	84.7
Ref. 13 (canted+twisted)[f]			1.13,1.04	93-96

[a]Structure with H-C-C-H dimers and dihydride units.
[b]Structure with alternating mono- and dihydride units.
[c]''Lean-to'' structure; see Fig. 2(b).
[d]''Herring-bone''-structure, see Fig. 2(a) and text.
[e]Substrate lattice constrained to (1×1) symmetry. Ideal structure (id.).
[f]Canted and twisted dihydride units.

the surface with respect to the surface layer and a (6×1) periodicity in the adsorbate layer. We obtain a dimer length of 1.548 Å, which is shorter than that observed in the $\theta=1$ structure. The contraction of the dimer bond, which increases the strain of the substrate lattice, is presumably driven by the need to reduce steric interactions between the dihydride units. A structure with alternating H-Si-Si-H dimers and SiH_2 dihydride units at a coverage of 1.33 ML has also been investigated by Northrup[29,27] and by Vittadini *et al.*[25] for the Si(100):1.33H (3×1) surface using *ab initio* calculations and was found to be stable at sufficiently high hydrogen partial pressures above the surface. On the basis of scanning tunneling microscopy, Boland[50] has also suggested the existence of a (3×1) phase on the hydrogenated Si(100) surface, presumably at coverages of $\theta=1.33$. We return to the relationship between the structures of Figs. 1(a) and 1(b) in Sec. V.

A third structure for the $\theta=1.5$ surface was found in,[10] in

which one hydrogen atom occupies a bridging position between each pair of surface carbon atoms. We find such a structure to be unstable. We suspect, though cannot prove, that the structure is a consequence of the fact that Davidson and Pickett fitted the C-H parameters to the forces in CH_4 rather than the energies, and thus overestimated the binding energy of a C–H bond.

The relief of steric interactions through distortion of the substrate lattice turns out to be more important than the simple contraction of the dimer bond in Fig. 1(b) just mentioned might suggest. For very high H coverages, one expects significant steric interactions between H atoms located on adjacent dihydride units. The most extreme case, that of the $\theta=2$ surface consisting solely of dihydride units, is generally considered to be thermodynamically unstable with respect to the $\theta=1$ surface for this very reason. Constraining the H atoms to lie in the ideal plane (i.e., the plane that passes through the surface C atoms and that lies perpendicular to that containing the back bonds of the substrate lattice), and relaxing all other atomic coordinates, we find that the H-C-H angle is reduced to 77.1° compared with the ideal tetrahedral angle of 109.4° (see Table III). Even so, H atoms on neighboring dihydride units are only 1.122 Å apart and significant steric interactions remain.

The case of the C(100) dihydride surface is considerably different from that of the Si(100) dihydride surface. Due to the larger lattice constant of Si, the shortest H-H distance between adjacent dihydride units is $R_{\text{H-H}}=$ 1.51 Å, even for the symmetric Si(100):2H (1×1) phase at a H-C-H angle of 102°. Here a simple canting of the SiH_2 units relative to the surface normal (with the H atoms remaining in the ideal plane) is sufficient to increase the H-H distance to 2.21 Å and to stabilize the dihydride phase.[29]

On the C(100):2H surface, the H-H repulsions can be relieved to some extent by twisting each dihydride unit out of the ideal plane. When we allow such a distortion, and perform a CG minimization with no constraints, we find that an energy minimum exists for a twist of 33.0°. The H-C-H angle thereby increases to 90.5°, and the energy is lowered by 1.353 eV/SS with respect to the previous zero-twist structure. The structure so obtained is similar to that of Yang and D'Evelyn,[6] who found a stable twist of 26.4°. On the other hand, other studies[4,5,10] found that twisting led to an overall increase in energy. Canted and/or twisted C(100):H structures have also been considered in the *ab initio* calculations of Zhang *et al.*[13] and Hong and Chou.[14] Hong and Chou found that a canting of the dihydride units by 11° with respect to the surface normal increases the H-H distances between different CH_2 groups from 1.10 Å to 1.44 Å and reduces the energy by 0.42 eV/SS. For the twisted configuration they calculated a stable twist angle of only 19°, leading to an only marginal energy gain of 0.01 eV/SS. The difference to our result comes from the fact that the twisted CH_2 units were constrained to be symmetric with respect to the C-C axis (for more geometrical details, see Table III). Zhang *et al.* considered a canted and twisted (2×1) structure generated by a molecular-dynamics simulation at 300 K and a subsequent steepest-descent quench. However, relative to the symmetric structure, an energy gain of only 0.12 eV/SS was achieved. This indicates that because of the rather low temperature and the very short duration of the simulation (0.02 ps) the global minimum for the dihydride structure has not been reached.

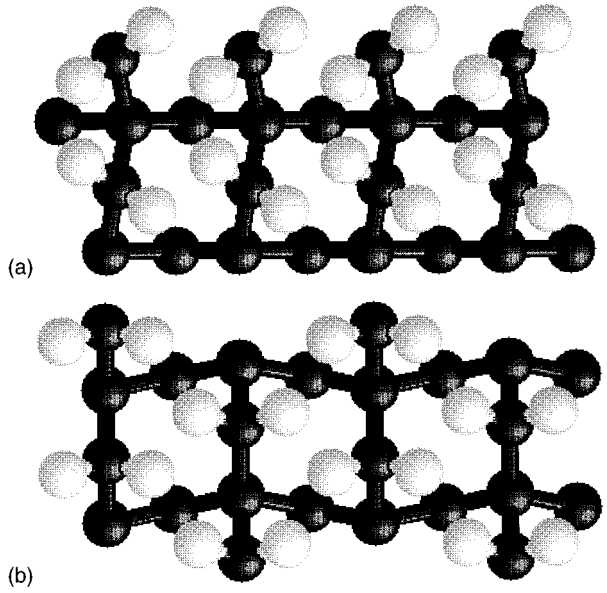

FIG. 2. Top views of (a) the ''herringbone'' and (b) the ''lean-to'' structures of C(100):2H, as obtained by CG minimization.

The relief of steric interactions in our twisted structure is achieved at the expense of deforming the preferred tetrahedral bonding at the surface C atoms. While the H-C-H angle lies closer to the ideal tetrahedral angle, other angles subtended at the surface C atoms become worse. In particular, the angles between the C–H bonds and the C–C backbonds are 96.4° and 137.0°. The situation can be improved by allowing the carbon substrate to relax away from the ideal (1×1) symmetry. We have in this way found two alternative structures for the $\theta=2$ surface that are more stable than those discussed so far. These structures were initially located by performing CG minimizations starting from partially disordered atomic configurations. Minimizations that start from an atomic configuration that assumes the ideal (1×1) symmetry cannot locate these lower-energy structures.

The first structure (the ''herringbone'' structure) is shown in Fig. 2(a). It may be derived from the ideal structure by shifting rows formed by second- and third-layer C atoms in alternate directions parallel to the [011] axis, while all other C atoms retain approximately ideal positions. Twisting of the dihydride units then leads to an approximately hexagonal array of H atoms, thus minimizing the steric repulsions. While the reduction in the steric interactions between H atoms is again achieved by twisting the dihydride units, the distortion of the underlying substrate leads to improved angles at the surface C atoms: the H-C-H angle is 94.3°, and the angles between the C–H bonds and the C–C backbonds are 98.4° and 129.9°. On the other hand, the deviation from ideal tetrahedral bonding is necessarily worse in deeper layers: the bond angles subtended at carbon atoms in the second and deeper layers range between 102.4° and 117.5°. The herringbone structure is found to be 0.390 eV/SS lower in energy than the simpler twisted structure that retains the (1×1) substrate lattice, and 1.743 eV/SS lower than the symmetric (1×1) dihydride surface. It is clearly energetically favorable to distribute the distortions from ideal tetrahedral

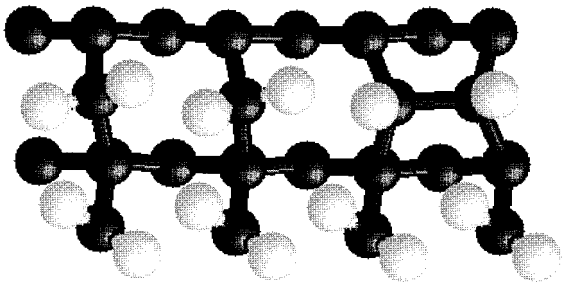

FIG. 3. Top view of the lowest-energy structure of C(100):1.75H, as obtained by CG minimization.

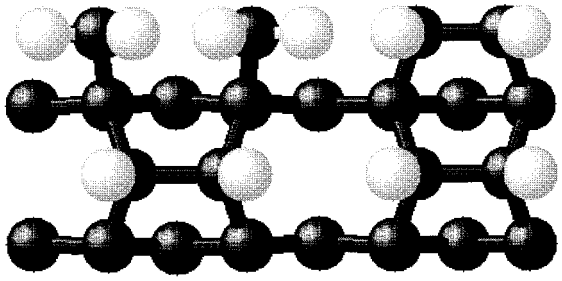

FIG. 4. Top view of the lowest-energy structure of C(100):1.25H, as obtained by CG minimization.

bonding, necessary to reduce steric repulsions, over a larger number of C layers.

The second structure (the ''lean-to'' structure), shown in Fig. 2(b), is obtained by shifting rows formed from first and second layer C atoms parallel to the $[0\bar{1}1]$ axis. In addition, the dihydride units lean over with respect to the ideal plane, leading again to an approximately hexagonal array of H atoms. The H-C-H angle is now 93.7°, the angles between the C–H bonds and the C–C backbonds are 103.1° and 123.6°, and the angles subtended at carbon atoms in the second and deeper layers range between 101.9° and 117.3°. The total energy is found to be 0.018 eV/SS lower than that of the herringbone structure, which marginal stabilization may be attributed to slightly improved angles subtended at the surface C atoms.

The lean-to and herringbone structures achieve a significant stabilization of the $\theta=2$ surface with respect to previously suggested structures. The distortion of the substrate lattice allows the formation of a hexagonal array of H atoms, thus minimizing the steric repulsion between adjacent H atoms, and relatively small deviations from ideal tetrahedral bonding. The energy gain achieved by admitting an unconstrained twisting of the dihydride units plus a deformation of the substrate is much larger than the modest energy gain of only 0.42 eV/SS (0.18 eV/SS) achieved by canting the CH_2 (SiH_2) units on the C(Si)(100):2H surface.[14,29] Hence we suspect that for Si(100) as well, the structures discussed here could be more stable than the simple canting models.

We would expect similar distortions to occur for other high-θ surfaces, and as an example we show in Fig. 3 the $\theta=1.75$ surface. As in the $\theta=1.5$ case, the surface consists of a mixture of dimer and dihydride units. Due to the higher concentration of dihydride units, however, there is a clear distortion of the substrate lattice. Because of the constraint imposed on the first layer carbon atoms by the dimer bond, this distortion takes a form similar to the herringbone structure of Fig. 2(a).

For the $\theta=1.5$ surface and lower H coverages, however, the strain energy associated with the distortion outweighs the reduction in steric interactions, and the substrate lattice remains undistorted. This is seen clearly for the $\theta=1.25$ surface shown in Fig. 4. In addition, the $\theta=1.33$ surface with alternating di- and monohydride units and (3×1) periodicity studied in Refs. 6,8, and 14 also conforms to the above pattern.

What implications do the above results have with regard to the LEED results discussed in the Introduction? The $\theta=1$ surface is traditionally associated with a (2×1) symmetry, and the $\theta=2$ surface with a (1×1) symmetry. The lean-to and herringbone structures shown in Figs. 2(a,b), however, possess a (2×1) symmetry. Therefore the (2×1) LEED pattern observed at low temperatures by a number of groups[16,18,20] simply indicates the existence of a long-range reconstruction of the surface, but is not sufficient to distinguish between the monohydrogenated and dihydrogenated surfaces.

Higher-order symmetries are predicted for certain coverages intermediate between $\theta=1$ and $\theta=2$. The $\theta=1.5$ surface shown in Fig. 1(b), for example, possesses a (4×1) symmetry, and the $\theta=1.33$ surface studied in Refs. 6 and 8 a (3×1) symmetry. An arbitrary fractional H coverage, however, is likely to consist of a disordered mixture of dimer and dihydride units. As suggested by Yang and D'Evelyn,[6] such a disordered surface structure would yield a (1×1) LEED pattern due to the underlying lattice. Hence, the (1×1) LEED pattern observed at low temperatures in Refs. 15–18 may indicate a disordered structure resulting from a surface that is not fully saturated by hydrogen.

Can we predict what H coverage should be stable at low temperatures by a comparison of the energies associated with different values of θ? The first problem is to decide on the form of excess hydrogen. In curve A of Fig. 5(a), we plot the total energy of the diamond slab plus a fixed amount of hydrogen as a function of θ, for which the excess hydrogen is assumed to exist as isolated H atoms. The $\theta=2$ surface, with the structure of Fig. 2(a) or 2(b), is clearly the most stable. In contrast, we plot in curve B of Fig. 5(b) the total energy assuming the excess hydrogen to exist in the form of H_2 molecules. The energetically most stable surface is now the $\theta=1.5$ structure shown in Fig. 1(b). The increase in total energy for coverages greater than $\theta=1.5$, which is reflected in curve A by a reduced rate of decrease of the total energy, probably indicates the onset of the distortion of the substrate lattice with the concomittant increase in strain energy.

Taking curves A and B of Fig. 5(a) together, it appears that the energetically most favorable system is the $\theta=1.5$ surface in contact with a gas of H_2 molecules. However, in the presence of a significant partial pressure of atomic hydrogen (generated for example by a hot filament), the equilibrium is likely to be shifted to higher coverages.

The picture emerging from Fig. 5(a), with a large adsorption energy for hydrogen up to monolayer coverage, and much lower energy gains for increased coverages, is consistent with the temperature-programmed desorption experi-

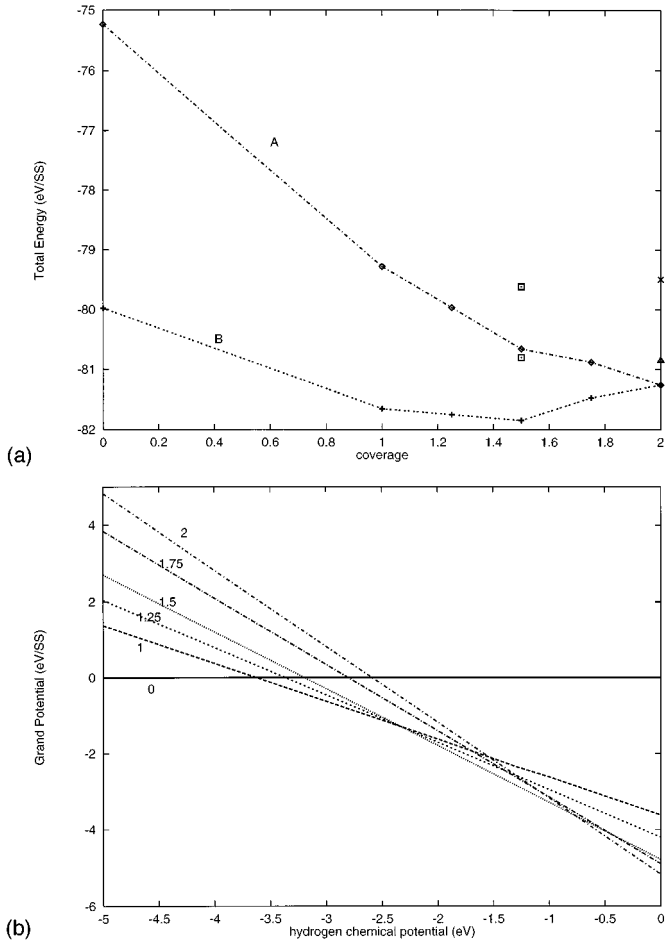

FIG. 5. (a) Total energy (in eV/SS) of the hydrogenated C(100) surfaces as a function of H coverage, with excess hydrogen in atomic (curve A) or molecular (curve B) form. Isolated points indicate additional metastable surfaces. (b) Grand potential Ω (in eV/SS) of the surfaces as a function of the chemical potential of atomic hydrogen μ_H (in eV). The coverage θ is indicated next to each line. The zero of the hydrogen chemical potential is taken as the value for the clean surface, namely $E-n_C\mu_C$.

ments of Hamza, Kubiak, and Stulen.[15] They found that H desorption from a very strongly H loaded C(100) surface occurs in a two-step process. The first desorption step has an activation energy of 1.61 eV per H atom and leads to a still H-covered surface with (2×1) symmetry. Further H desorption requires much higher activation energies. From Fig. 5(a) we find that the desorption processes reducing the coverage from $1.5<\theta<2$ to about $\theta\sim1$ require activation energies of 1.5 to 1.9 eV, in good agreement with the desorption experiment[15] and the *ab initio* predictions,[12] whereas the activation energies increase steeply at lower coverages. In the presence of a reservoir of hydrogen atoms above the surface, the stability is determined by the grand potential Ω given at zero temperature by (neglecting the zero-point energies; cf. Ref. 14)

$$\Omega = E - n_C\mu_C - n_H\mu_H, \tag{3}$$

where E is the total energy and n_C and n_H are the numbers of C and H atoms. The zero-point energies associated with the vibrations of the light hydrogen atoms are generally quite

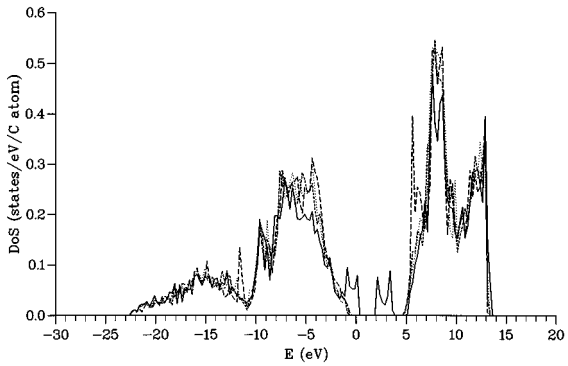

FIG. 6. Density of electronic states (in states/eV/carbon atom) as a function of energy E (in eV) for the lowest-energy C(100) (solid curve), C(100):H (short-dashed curve), C(100):1.5H (dotted curve), and C(100):2H (long-dashed curve) surfaces. E_F marks the Fermi energy for all surfaces.

large (0.27 eV/H atom in the H_2 molecule). However, for the present case only the differences in the zero-point energies in different systems are important. Even if we assume that these differences can be as large as 10%, they are still much too small to influence the energetics depending on the coverage. In our case the chemical potential μ_C is equal to its value in bulk diamond, and the number of C atoms is constant. The number of hydrogen atoms varies with the coverage. Hence the range of stability of phases with different H coverages is determined by the chemical potential μ_H of hydrogen. Figure 5(b) shows the grand potential as a function of μ_H for the different coverages considered. We find that for $\mu_H<-3.6$ eV, the clean C(100)-(2×1) surface has a lower potential than any of the H-terminated surfaces. In the range -3.6 eV$<\mu_H<-2.3$ eV the (2×1) monohydride surface is thermodynamically stable, followed for -2.3 eV $<\mu_H<-0.8$ eV by the $\theta=1.5$ surface, and at still higher values of the chemical potential the dihydride phase is lowest in energy. For intermediate coverages around $\theta=1.25$ and $\theta=1.75$, the grand potential is always higher than or at most equal to that for 1, 1.5, or 2 ML coverage so that the ordered phases turn out to be unstable. However, in this case a disordered distribution of dimers and dihydride units could lead to an entropic stabilization of phases with intermediate coverages.

IV. ELECTRONIC STRUCTURE

As outlined in Sec. II, the total and partial electronic densities of state are readily obtainable from the diagonalization of H_{TB}. The predicted electronic structure is expected to be reasonable in the valence band and the lower half of the conduction band: in the upper half of the conduction band, the contribution from higher-energy basis states, not included in the present work, is likely to be significant. In fact, it was for this reason that Gavrilenko[9] included an additional s^* state in his basis.

In Fig. 6, we plot the total DOS for coverages $\theta=0$, 1, 1.5 (dimerized structure), and 2 (lean-to structure). The overall form of each spectrum in similar, due to the constant contribution from bulk electronic states. In the valence band, the s-like and p-like subbands are clearly distinguished, together

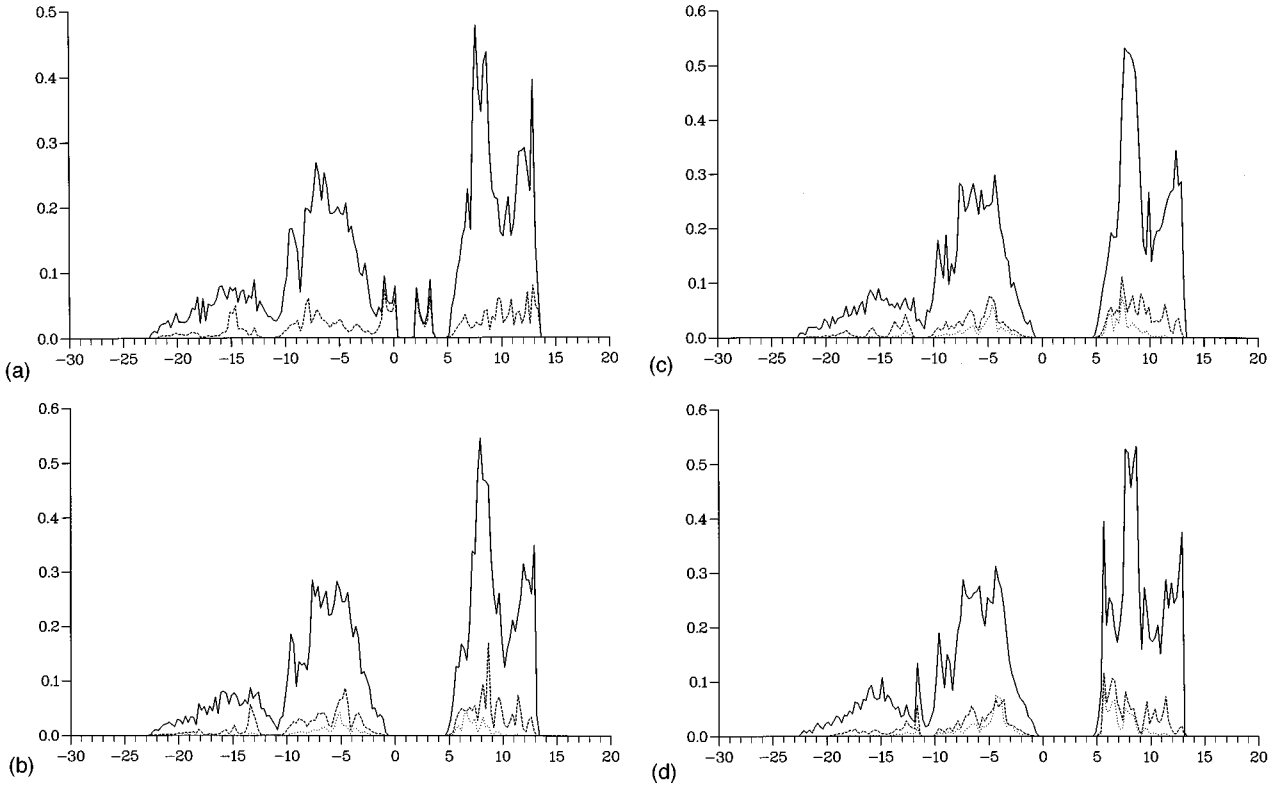

FIG. 7. DOS and partial DOS for the lowest-energy (a) C(100), (b) C(100):H, (c) C(100):1.5H, and (d) C(100):2H surfaces. The solid curve gives the total DOS, the dashed curve gives the contribution from surface C atoms, and the dotted curve the contribution from H atoms. E_F marks the Fermi energy for all surfaces. The units are as in Fig. 6.

with the characteristic peak arising from their overlap. The differences observed reflect changes wrought by the adsorbed hydrogen, particularly on surface states. These changes are most easily understood with reference to the partial DOS which are plotted in Figs. 7(a–d).

The most striking difference between the plots shown in Fig. 6 is the existence of states in the bulk band gap for $\theta=0$. Figure 7(a) shows that the DOS of these gap states is almost entirely accounted for by the contribution from surface C atoms, and so the gap states can be classified as surface states. On the reconstructed clean C(100) surface, each dimer unit is associated with two dangling bonds, which mix to give occupied π and unoccupied π^* states (although addition of electron correlation effects may alter this simple picture.[3]) The π and π^* states can be identified with the peaks observed in the ranges $-1\rightarrow 0$ eV and $2\rightarrow 4$ eV respectively. Interactions between different dimers within a dimer row lead to the observed broadening. These observations accord closely with the results of previous studies[8,10–12,49] and with the photoemission studies.[21–23]

On hydrogenation to a coverage $\theta\geqslant 1$, the gap states disappear and additional states are observed in the energy ranges $-7\rightarrow -3$ eV and $7\rightarrow 8$ eV. The resulting band gap lies very close to the experimental bulk gap of 5.5 eV, indicating the bonding and antibonding surface states have been shifted by sufficiently large energies to fall into the region of the bulk valence and conduction bands. (Note that as the TB Hamiltonian has been adjusted to reproduce the experimentally measured gap, hence our predictions do not suffer the usual shortcoming of the local-density approximation of producing too narrow gaps.) These predictions are in excellent agreement with the photoemission intensities of Graupner *et al.*[22] and Francz and Oelhafen,[23] showing a decrease of the photemission intensity for $-2\rightarrow 0$ eV and an increase in the range $-6\rightarrow -3$ eV. The absence of surface states in the bulk gap is in contrast to the electronic structure of geometries that possess isolated monohydride units. In such a case, the dangling bonds associated with the monohydride units give rise to gap states. For example, both Davidson and Pickett[10] and Furthmüller *et al.*[11,12] assumed structures for the $\theta=1.5$ surface consisting of alternating rows of dihydride and monohydride units, and consequently observed well-defined peaks in the band-gap region.

For the $\theta=2$ spectrum additional states are observed on either side of the band gap. The most pronounced feature is a very intense empty surface state immediately at the bottom of the conduction band, and a further increase of the DOS in the range -5 eV <-3 eV. These additional states are also observed for the herringbone and the simple twisted structures, but *not* for the $\theta=2$ surface in which the dihydride units are constrained in the untwisted configuration. From the partial DOS shown in Fig. 7(d), we see that these states have a significant contribution from the hydrogens and the surface carbon atoms, and their appearance presumably reflects the changes due to the twisting of the dihydride units.

Altogether we find that the present results agree perfectly well with the observed changes in the photoelectron spectra as a function of the hydrogen coverage.

V. DYNAMICAL SIMULATIONS OF SURFACE RECONSTRUCTIONS

We showed above that, for the present model, it is energetically unfavorable for monohydride units to occur in iso-

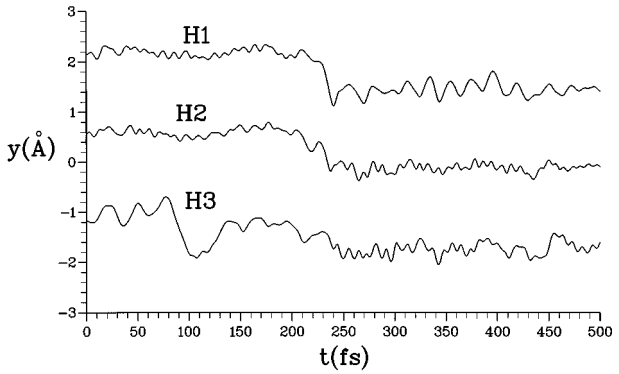

FIG. 8. Trajectories of three H atoms during the TBMD run described in the text. The y coordinates of atoms H1, H2, and H3 (see Fig. 1) in angstroms are plotted as a function of simulation time in femtoseconds. A clear transition is visible at $t \sim 230$ fs.

lation. To test whether isolated monohydride units can survive as metastable states under CVD conditions, we ran a TBMD simulation at 1200 K starting from the atomic configuration shown in Fig. 1(a). In Fig. 8, we plot the y coordinates of the three H atoms labeled in Fig. 1(a) as a function of time. The plot shows that the atoms at first oscillate around their initial positions, but a clear transition is seen around $t=230$ fs. A similar transition occurs around $t=150$ fs for the adjacent row of H atoms, and the final structure is as shown in Fig. 1(b).

The transition observed involves the migration of atom H2 between neighboring surface C atoms, with the simultaneous formation of a surface dimer. The required rearrangement is in fact minor: atom H2 moves through a total distance of only 0.67 Å. Nevertheless, it brings a gain in energy of 1.036 eV/SS (eight-layer slab) due to the removal of the dangling bonds associated with the monohydride units.

We conclude that, at hydrogen coverages $\theta > 1$, isolated monohydride units are unstable. The diffusion of the H atoms of the C(100) surface is sufficiently fast to lead very quickly to the recombination of the monohydride units to form H-C-C-H dimers.

VI. CONCLUSIONS

We have presented a detailed study of the structural and electronic properties of clean and hydrogenated C(100) surfaces using tight-binding molecular dynamics based on an accurate and transferable tight-binding Hamiltonian. For the clean surface and for hydrogen coverages up to a monolayer, our results are in very good agreement with *ab initio* local-density-functional calculations.[2,11–14,49] At higher coverages, the efficiency of the TB-MD technique allows for dynamical simulations of rather large ensembles and this has led to the following results. (a) At coverages $1 < \theta < 2$, isolated monohydride units are found to be unstable. The mobility of the adsorbed hydrogen atoms is large enough to lead very quickly to a ''recombination'' of isolated monohydride units via the formation of H-C-C-H surface dimers. At these coverages, the structure of the surface is probably determined by a disordered arrangement of dihydride units and surface dimers, leading to an overall (1×1) pattern in a LEED experiment, as observed. The recombination of the monohydride units in surface dimers with saturated bonds also explains the absence of dangling-bond surface states, in agreement with the photoemission studies on C(100) surfaces exposed to high doses of atomic hydrogen. (b) As for the Si(100) surface,[29,27] it is possible to saturate all dangling bonds at the C(100) surface with hydrogen, leading to a coverage of $\theta=2$. However, unlike for Si(100), a simple canting of the CH_2 units in the ideal plane is not sufficient to stabilize the C(100):2H surface. A larger energy gain can be achieved by twisting the CH_2 groups out of the plane, as proposed by Yang and D'Evelyn,[6] but contradicting previous semiempirical studies[4,5] and also the recent TB calculations of Davidson and Pickett.[10] However, we find that although the twisting of the CH_2 groups reduced steric repulsions, it increases the elastic strains in the substrate. Allowing the substrate to relax from the imposed (1×1) symmetry leads to two energetically nearly degenerate surface structures with still lower energies. In both structures, the adsorbed H atoms form slightly distorted honeycomb layers; they only differ by shifted adjacent rows of C atoms in different directions. (c) With these structures, hydrogen coverages of up to $\theta=2$ are stable against the desorption of atomic hydrogen. The stability of the different surfaces as a function of the chemical potential of H above the surface has been studied, and we predict that with increasing μ_H, C(100)-(2×1), C(100):H-(2×1), C(100):1.5H-(4×1), and C(100):2H-(2×2) phases should be observed (this refers to a homogeneous coverage). (d) Electronic surface states are observed for the clean C(100) surface, but disappear completely at a monolayer coverage of H. At higher coverages, isolated monohydride units lead to a reappearence of gap states. However, for all relaxed hydrogenated C(100) surfaces with no isolated monohydride units, there are no electronic surface states in the bulk gap. The observed changes of the electronic DOS as a function of hydrogen coverage are now in perfect agreement with the photoemission observations.

ACKNOWLEDGMENTS

This work was supported by the Austrian Science Foundation (Fonds zur Förderung der wissenschaftlichen Forschung) under Projects No. M0181-PHY and No. S5908-PHY within the German-Austrian-Swiss research cooperation D-A-CH on ''Superhard materials.'' M.D.W. would like to thank Jürgen Furthmüller for useful discussions. M.D.W. is also grateful to the Royal Commission for the Exhibition of 1851 for the grant of a leave of absence.

*Present address: Daresbury Laboratory, Daresbury, Warrington WA4 4AD, England. Electronic mail: m.d.winn@dl.ac.uk

[1] W. A. Yarbrough and R. Messier, Science **247**, 688 (1990).
[2] P. Krüger and J. Pollmann, Phys. Rev. Lett. **74**, 1155 (1995).
[3] B. Weiner, S. Skokov, and M. Frenklach, J. Chem. Phys. **102**, 5486 (1995).
[4] S. P. Mehandru and A. B. Anderson, Surf. Sci. **248**, 369 (1991).
[5] X. M. Zheng and P. V. Smith, Surf. Sci. **256**, 1 (1991).

[6] Y. L. Yang and M. P. D'Evelyn, J. Am. Chem. Soc. **114**, 2796 (1992); J. Vac. Sci. Technol. A **10**, 978 (1992).
[7] Th. Frauenheim, U. Stephan, P. Blaudeck, D. Porezag, H. G. Busmann, W. Zimmermann-Edling, and S. Lauer, Phys. Rev. B **48**, 18 189, (1993).
[8] S. H. Yang, D. A. Drabold, and J. B. Adams, Phys. Rev. B **48**, 5261 (1993).
[9] V. I. Gavrilenko, Phys. Rev. B **47**, 9556 (1993).
[10] B. N. Davidson and W. E. Pickett, Phys. Rev. B **49**, 11 253 (1994).
[11] J. Furthmüller, J. Hafner, and G. Kresse, Europhys. Lett. **28**, 659 (1994).
[12] J. Furthmüller, J. Hafner, and G. Kresse, Phys. Rev. B **53**, 7334 (1996).
[13] Z. Zhang, M. Wensell, and J. Bernholc, Phys. Rev. B **51**, 5291 (1995).
[14] S. Hong and M.Y. Chou (unpublished).
[15] A. V. Hamza, G. D. Kubiak, and R. H. Stulen, Surf. Sci. **237**, 35 (1990).
[16] R. E. Thomas, R. A. Rudder, and R. J. Markunas, J. Vac. Sci. Technol. A **10**, 2451 (1992).
[17] S. T. Lee and G. Apai, Phys. Rev. B **48**, 2684 (1993)
[18] V. S. Smentkowski, H. Jänsch, M. A. Henderson, and J. T. Yates, Surf. Sci. **330**, 207 (1995).
[19] R. E. Stallcup, A. F. Aviles, and J. M. Perez, Appl. Phys. Lett. **66**, 2331 (1995).
[20] B. D. Thoms and J. E. Butler, Surf. Sci. **328**, 291 (1995).
[21] J. Wu, R. Cao, X. Yang, P. Pianetta, and I. Lindau, J. Vac. Sci. Technol. A **11**, 1048 (1993).
[22] R. Graupner, J. Ristein, and L. Ley, Surf. Sci. **320**, 193 (1994).
[23] G. Francz and P. Oelhafen, Surf. Sci. **329**, 193 (1995).
[24] J. Dabrowski and M. Scheffler, Appl. Surf. Sci. **56**, 15 (1992).
[25] A. Vittadini, A. Selloni, R. Car, and M. Casarin, Phys. Rev. B **46**, 4348 (1992).
[26] M. Rohlfing, P. Krüger, and J. Pollmann, Phys. Rev. B **52**, 13 753 (1995).
[27] J. E. Northrup, Phys. Rev. B **47**, 10 032 (1993).
[28] M. Needels, M. C. Payne, and J. D. Joannopoulos, Phys. Rev. Lett. **58**, 1765 (1987).
[29] J. E. Northrup, Phys. Rev. B **44**, 1419 (1991).
[30] T. Sakurai and H. D. Hagstrum, Phys. Rev. B **14**, 1593 (1976).
[31] Y. J. Chabal and K. Raghavachari, Phys. Rev. Lett. **54**, 1055 (1985).
[32] S. Skokov, B. Weiner, and M. Frenklach, J. Phys. Chem. **98**, 7073 (1994).
[33] C. Z. Wang, C. T. Chan, and K. M. Ho, Phys. Rev. B **39**, 8586 (1989).
[34] A. P. Sutton, M. W. Finnis, D. G. Pettifor, and Y. Ohta, J. Phys. C **21**, 35 (1988).
[35] L. Goodwin, A. J. Skinner, and D. G. Pettifor, Europhys. Lett. **9**, 701 (1989).
[36] D. G. Pettifor, Phys. Rev. Lett. **22**, 2480 (1989).
[37] C. W. Gear, *Numerical Initial Value Problems in Ordinary Differential Equations* (Prentice Hall, Englewood Cliffs, NJ, 1971).
[38] A. Arnold, N. Mauser, and J. Hafner, J. Phys. Condens. Matter **1**, 965 (1989).
[39] C. Z. Wang, K. M. Ho, and C. T. Chan, Phys. Rev. B **47**, 14 835 (1993); Phys. Rev. Lett. **70**, 611 (1993); Phys. Rev. B **50**, 12 429 (1994).
[40] R. Virkunnen, K. Laasonen, and R. M. Nieminen, J. Phys. Condens. Matter **2**, 1537 (1990).
[41] L. Goodwin, J. Phys. Condens. Matter **3**, 3869 (1991).
[42] C. H. Xu, C. Z. Wang, C. T. Chan, and K. M. Ho, J. Phys. Condens. Matter **4**, 6047 (1992).
[43] M. D. Winn and M. Rassinger (unpublished).
[44] D. A. Papaconstantopoulos, *Handbook of the Band Structures of Elemental Solids* (Plenum, New York, 1986).
[45] W. Kolos and L. Wolniewicz, J. Chem. Phys. **41**, 3663 (1964).
[46] Y.Wang and C. H. Mak, Chem. Phys. Lett. **235**, 37 (1995).
[47] *CRC Handbook of Chemistry and Physics*, 75th ed. (CRC Press, Boca Raton, FL, 1994).
[48] H. J. Monkhorst and J. D. Pack, Phys. Rev. B **13**, 5188 (1976).
[49] C. Kress, M. Fiedler, W. G. Schmidt, and F. Bechstedt, Phys. Rev. B **50**, 17 697 (1994).
[50] J. J. Boland, Surf. Sci. **261**, 17 (1992).